Journal of Applied Electrochemistry (2005) 35:327–337
DOI 10.1007/s10800-004-7471-2

On efficiency of both single fuel cells and stacks I

ROBERTO C. DANTE[1,*], JOCHEN LEHMANN[2] and OMAR SOLORZA-FERIA[3]
[1]*Renewable Energy Center, Basic Sciences Department, Engineering Division, Instituto Tecnológico de Monterrey, at Mexico City, Calle del Puente 222, Col. Ejidos de Huipulco, 14380, Mexico City*
[2]*Electrical Techniques Faculty, Fachhochschule Stralsund (University of Applied Sciences), Zur Schwedenschanze 15, 18435, Stralsund, Germany*
[3]*Chemistry Department, Centro de Investigaciones y Estudios Avanzados (CINVESTAV), Instituto Politécnico Nacional, Av. Instituto Politécnico Nacional 2508 Col. San Pedro Zacatenco, 07360, Mexico City*
*(*author for correspondence, fax: +52-55-54832163, e-mail: rdante@itesm.mx)*

Received 6 July 2004; accepted in revised form 2 December 2004

Key words: fuel cell efficiency, fuel cell thermodynamics, polarization curve, stack reaction extent, stack utilization

Abstract

A method to estimate the efficiency of a stack of several identical cells is described on the basis of the electrochemical behavior of a single cell. Efficiency of fuel cell stacks is defined by means of a combination of semi-empirical models of polarization curves and dimensionless variables such as reaction extent and utilization. The connection of flows among the cells is basically divided in two extreme cases and one intermediate case. Higher efficiencies are obtained when the same main flow (both anodic and cathodic) passes consecutively through the stack cells (Chain Flow), because it is favored thermodynamically. It is less favored when the main flow is strictly divided among all the cells (Separate Flow). In the intermediate case, the main flow is divided among all the stack cells and all the outlets are collected in one flow. The latter can spontaneously evolve to the more thermodynamically stable behavior of Chain Flow.

List of the principal symbols

$\dot{n}_{qj}$	Flow rate of the reagent j in the q-th cell (mol s^{-1})
$\dot{n}_{ql}$	Flow rate of the limiting reagent l in the q-th cell (mol s^{-1})
u_{qj}	Utilization of the reagent j in the q-th cell
u_q	Utilization of the limiting reagent l in the q-th cell
$\dot{H}_p$	Enthalpy flow rate of the product p (J mol^{-1})
$\dot{H}_r$	Enthalpy flow rate of the reagent r (J mol^{-1})
$\dot{W}_{el,irr}$	Irreversible electrical power of the fuel cell stack (J s^{-1})
i	Current density (A cm^{-2})
A_q	Active area of the q–th cell (cm^2)
U_q	Potential of the q–th cell (V)
U_{1q}	Potential part depending on reaction extent of the q-th cell (V)
U_{2q}	Potential part depending on partial pressures of the q-th cell (V)
p_{qj}	Partial pressure of the reagent j in the q-th cell (kPa)
$p^s{}_{qj}$	Surface partial pressure of the reagent j in the q-th cell (kPa)
u_{sn}	Stack utilization
n	Total number of cells of the stack
c	Number of moles of electrons exchanged (Equation 7) (mol)
F	Faraday constant (96501 C mol^{-1})
$\overline{U}$	Stack average potential (V)
k_j	Constant for reagent j in Equation 12.5 and 12.6
$U(0)$	Single cell potential at a reaction extent of 0 (V)
ΔH°	Standard enthalpy of fuel cell reaction. For water formation: $\Delta H° = -285.5$ k J mol^{-1}
ΔG°	Standard Gibbs free energy of fuel cell reaction. For water formation: $\Delta G° = -237.2$ k J mol^{-1}
U_H	Potential determined using enthalpy: $U_H = \Delta H/cF$. For water formation in standard conditions: $U_H =$ 1.48 V

Greek letters

η	Efficiency of fuel cells
$\dot{\xi}_q$	Reaction rate in the q-th cell (s^{-1})
ξ_q	Reaction extent of the q-th cell
ξ_{sn}	Stack reaction extent
ν_j	Stoichiometric coefficient of the reagent j (mol)
ν_l	Stoichiometric coefficient of the limiting reagent l (mol)
α^q_{lj}	Time interval difference between the limiting reagent l and the reagent j (s)
α_1, α_2, α_3, α_4, α_6	Parameters of Equations 12–12.4 and 13 depending on temperature, on flow rates and on pressures of the first cell (V)
α_5	Parameter of the exponential term in Equations 12–12.3 and 13

1. Introduction

The efficiency of the water formation reaction is very easily defined in standard conditions [1]:

$$\eta = \frac{\Delta G^0_{H_2O}}{\Delta H^0_{H_2O}} = \frac{-237.2\ \mathrm{kJ\,mol^{-1}}}{-285.5\ \mathrm{kJ\,mol^{-1}}} = 0.83. \quad (1)$$

This efficiency is the Gibbs free energy efficiency of the reaction. It does not deal with kinetic aspects which can lead the reaction far from equilibrium; moreover, both reversible processes and transformations are constantly taken into account.

An efficiency of thermal machines, based on the Carnot cycle, is defined in the following way [1]:

$$\eta = \frac{(\Delta Q_{in} - \Delta Q_{out})_{rev}}{(\Delta Q_{in})_{rev}} = 1 - \frac{T_1}{T_2}, \quad (2)$$

$(\Delta Q_{in})_{rev}$ being the reversible heat coming into the system and the difference $(\Delta Q_{in} - \Delta Q_{out})_{rev}$ the reversible work delivered by the system; T_2 is the highest temperature of the cycle and T_1 the lowest temperature.

Ayoub Kazim [2] gives a general definition for fuel cell efficiency, starting from flows of thermodynamic quantities [3] as indicated in the following equations:

$$\eta = \frac{\text{Electrical Output}}{(X)_R - (X)_P}, \quad (3)$$

$$\eta = \frac{\dot{W}_{el}}{(\dot{X}_{air,R} + \dot{X}_{H_2,R}) - (\dot{X}_{air,P} + \dot{X}_{H_2O,P})}, \quad (4)$$

where $\dot{X}_{air,R}$ and $\dot{X}_{H_2,R}$ are the rates of some specified thermodynamic quantities (e.g. enthalpy or exergy) of the reagents (oxygen in air and hydrogen) , and on the other hand, $\dot{X}_{air,P}, \dot{X}_{H_2O,P}$ (water and products like water in air) are the thermodynamic quantity rates of products, and $\dot{W}_{el}$ is the electrical power output. This definition is based on the operating parameters of fuel cells, where time dependence and flow rates dominate performance. It includes physical and chemical thermodynamic forces as well. These efficiency definitions reflect the conditions of reagents and products in fuel cell operations, and lead to efficiencies with realistic values: in the range 0.3–0.4 for a 10 kW fuel cell stack, using also ideal gas equations for both physical exergies and entropies of mixed products [2, 4].

Its emphasis on time dependent or steady variables (flow rates of both reagents and products, flow rates of exergies or enthalpies and power) represents an important step in the efficiency statements of fuel cell systems.

Some of the classic methods used to calculate fuel cell efficiency are the so-called: Electrochemical, Faradaic and Practical efficiencies [5], which, combined in a steady operational way, would give [6]:

$$\eta = \frac{\dot{W}_{el,irr}}{(\dot{H}_P - \dot{H}_R)_{rev}}, \quad (5)$$

where $\dot{H}_P$ and $\dot{H}_R$ are respectively the reversible enthalpy flow rates of products and reagents (Kazim uses the opposite convention with respect to the sign of thermodynamic functions and uses exergies instead of enthalpies), while $\dot{W}_{el,irr}$ is the irreversible power output of the fuel cell, which usually will be irreversible. Working with enthalpy connects directly to thermal energy and heat, which allows a direct comparison with the classical Carnot efficiency.

The efficiency of a single cell can be different from that of a whole stack, depending on reagent utilization. Irreversible processes are involved in most cases; e.g. Equation 2 deals only with reversible processes, and Equation 5 is often a hybrid of an irreversible numerator and a reversible denominator. The main objective is to present a way to predict and model fuel cell stack efficiencies, starting from single cells and ending with large stacks of several identical cells up to so large stacks, these are considered infinite. The efficiency definition of Equation 5 is used, which combines some operative aspects, evidenced by Kazim [2], and other definitions [4]. The focus of the discussion is on the linkage between a single cell and a stack, made of a series of cells identical to the initial single cell. Only the case of steady conditions is considered, implying that all rates are constant and leading actually to time independent equations. A large segment of our results is semi-quantitative predictions, due to approximations, such as, neglecting friction of gases in the flow fields. However, the conclusions are of general validity, for example, the efficiency trend of Proton Exchange Membrane (PEM) fuel cell stacks with different kinds of flow. This work represents the first part in a series of two works. The first part focuses on general definitions and model development. Conclusions regarding the effects of both kinds of flow, and the number of cells, on the efficiency of fuel cell stacks are obtained. The second part focuses mainly on the comparison between model predictions and experimental results.

2. Methodology and models

Our starting point is the definition of two basic types of flow. In the first case, hydrogen and air (or oxygen) pass through each cell consecutively, generating a chain or serial connection of flows (Chain Flow stack, case (a) in Figure 1); such a flow provides the proper steps useful for thermodynamics. In the second case, feeding of each cell comes separately from the same main stream (Separate Flow stack, case (b) in Figure 1) and will be approached using thermodynamic conclusions and results from our first case. The Separate Flow case will be discussed in Subsection 4.3. This section will deal only with Chain Flow.

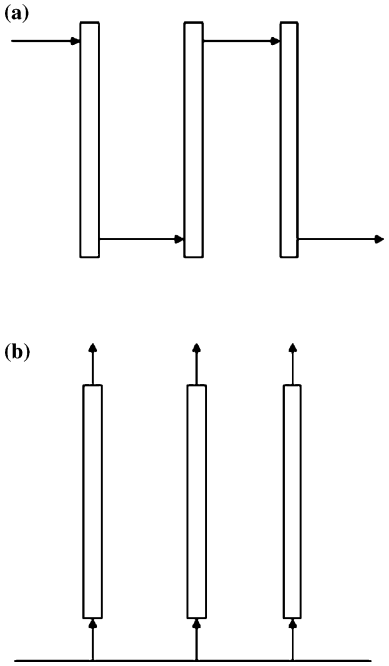

Fig. 1. (a) (Chain feeding): the same stream passes initially in the first cell and then in the second, and so on; (b) (Separate feeding): the main gas stream is divided into secondary streams each one feeding a different cell. Each cell is represented by a box and each stream by an arrow.

The dimensionless variable utilization u will be the fundamental tool used to forecast cell potential and correlate it with flow rates in the *q-th* cell:

$$u_{qj} = \frac{\dot{n}_{qj} - \dot{n}_{q+1,j}}{\dot{n}_{qj}}. \tag{6}$$

In Equation 6, j is the reagent j, e.g. hydrogen or oxygen in our case, n_{qj} and $\dot{n}_{q+1,j}$ are the inlet molar flow rate and the outlet flow rate of reagent j for the *q-th* cell of a stack, respectively.

Utilization has a direct connection with current density i through the following equation:

$$u_{qj} = \frac{iA_q}{(c/v_j)\dot{n}_{qj}F}, \tag{7}$$

where F is the Faraday constant, A_q the active area of the *q-th* cell, c the number of exchanged electrons per mol of product and v_j the stoichiometric coefficient of the reagent j [7]. Polarization curves of single cells show the potential variation with current density. The usual variable i is changed to the dimensionless variable utilization u. Utilization can be related to the reaction extent by means of the reaction rate

$$\dot{\xi}_q = -\frac{\dot{n}_{q+1,j} - \dot{n}_{qj}}{v_j} = u_{qj}\left(\frac{\dot{n}_{qj}}{v_j}\right). \tag{8}$$

The relationship between reaction rate and current density is obtained combining Equation 8 with Equation 7:

$$\dot{\xi} = \frac{iA_q}{cF}. \tag{9}$$

If the active area A_q is the same for each cell, then the reaction rate, $\dot{\xi}$, will also be the same for each cell, (Equation 9).

The reaction extent can be expressed in a useful form, depending on the q-th cell and equal to the utilization of the limiting reagent l of the q-th cell, in the following way:

$$\xi_q = \dot{\xi}\left(\frac{v_j}{\dot{n}_{qj}} + \alpha^q_{lj}\right) = u_{ql}, \tag{10}$$

where the term α^q_{jl} corresponds to the difference between the time intervals $v_j/\dot{n}_{q,j}$ of the limiting reagent l and the considered reagent j:

$$\frac{v_l}{\dot{n}_{ql}} - \frac{v_j}{\dot{n}_{qj}} = \alpha^q_{lj}. \tag{11}$$

The appropriate thermodynamic variable should be better chosen as the reaction extent ξ_q, i.e. the utilization of the limiting reagent.

The cell potential, U_q, depends on the current density and, experimentally, this dependence is reported in the polarization curves [8]. There are several semi-empirical models describing polarization curves; one of the most common is that proposed by Kim et al. [9] and Springer et al. [10], where the reaction extent, instead of current density, and partial pressures are introduced as the independent variables [7, 11]:

$$U_q(\xi_q, p_{qj}, T) = U_{1q}(\xi_q, T) + U_{2q}(p_{qj}, T), \tag{12.1}$$

$$U_q(\xi_q, p_{qj}, T) = \alpha_1 - \alpha_2\xi_q - \alpha_3 \ln \xi_q - \alpha_4 \exp \alpha_5\xi_q + \alpha_6 \ln \prod_j \left(p_{qj}/p_{1j}\right)^{v_j}, \tag{12.2}$$

$$U_{1q}(\xi_q, T) = \alpha_1 - \alpha_2\xi_q - \alpha_3 \ln \xi_q - \alpha_4 \exp \alpha_5\xi_q, \tag{12.3}$$

$$U_{2q}(p_{qj}, T) = \alpha_6 \ln \prod_j \left(p_{qj}/p_{1j}\right)^{v_j}, \tag{12.4}$$

$$p^s_{qj} = k_j p_{qj}, \tag{12.5}$$

$$p^s_{1j} = k_j p_{1j}, \tag{12.6}$$

In Equation 12.1 the cell potential U_q is divided into two parts: U_{1q} (Equation 12.3) depends on the cell reaction extent ξ_q and U_{2q} (Equation 12.4) depends on cell partial pressures p_{qj}. Equation 12.1 takes the form of Equation 12.2 when Equations 12.5–12.6 are satisfied simultaneously. Equations 12.5 and 12.6 say that the pressure of the reagent j on the electrode surface p^s_{qj} is proportional to the nominal pressure. The same behavior is also guessed to be valid for the reference surface pressure of the reagent j, p^s_{1j}, so that it is unnecessary to know the surface pressure with such definitions (Equations 12.5–12.6).

The coefficients k_j of Equations 12.5 and 12.6 disappear in Equations 12.2 and 12.4, because they are present in both the numerator and the denominator of the logarithmic term. The introduction of reaction extent in Equation 12.2, instead of the common current density is based, on the fact that reaction extent is proportional to utilization (Equation 10), which is proportional in turn to current density (Equation 7). Reaction extent has the advantage of linking directly to thermodynamics, and therefore to the grade of irreversibility of the process.

The reference polarization curve, obtained from one single cell, is:

$$U(\xi, p_{1j}, T) = \alpha_1 - \alpha_2\xi - \alpha_3 \ln \xi - \alpha_4 \exp \alpha_5\xi, \qquad (13)$$

where the α_i parameters (Equations 12.2–13) depend on T and $p_{1j,}$ Equation 13 is essentially U_{1q} of Equation 12.2.

3. The reversible stack

The equilibrium conditions imply that $\dot{\xi} \to 0$ so that for each cell $\dot{\xi} \to 0$, according to Equation 10. Electrochemical stacks are discussed in which the outlet of one cell is the inlet of the next cell, which will be called a Chain Flow stack, as indicated in case (a) of Figure 1. The utilization of each cell is related directly to the utilization of the previous one.

Three identical serial cells are considered, where the flow rates of the limiting reagent for each cell are: $\dot{n}_{1l} = a, \dot{n}_{2l} = b, \dot{n}_{3l} = c$; the utilization definitions of every cell (u_{1l}, u_{2l}, u_{3l}) and that of the whole stack (u_{s3}) are reported here:

$$u_{1l} = \frac{a-b}{a} = 1 - \frac{b}{a}, \qquad (14.1)$$

$$u_{2l} = \frac{b-c}{b} = 1 - \frac{c}{b}, \qquad (14.2)$$

$$u_{3l} = \frac{c-d}{c} = 1 - \frac{d}{c}, \qquad (14.3)$$

$$u_{s3} = \frac{a-d}{a} = \frac{(a-b)+(b-c)+(c-d)}{a} = \frac{au_{1l} + bu_{2l} + cu_{3l}}{a}. \qquad (14.4)$$

Starting from Equations 14.1–14.4 we can easily obtain the following equation:

$$u_{s3} = u_{1l} + (1-u_{1l})u_{2l} + (1-u_{1l})(1-u_{2l})u_{3l}, \qquad (15)$$

for a stack of n cells, Equation 15 turns in:

$$u_{sn} = u_{1l} + \sum_{q=2}^{n} u_{ql}\left[\prod_{p=1}^{q-1}(1-u_{pl})\right] = \xi_{sn}, \qquad (16)$$

where ξ_{sn} is the stack reaction extent and coincides with u_{sn} which is defined on the limiting reagent l in order to be coherent with the definition of Equation 10.

If the reversible conditions are satisfied: $i \to 0, \dot{\xi} \to 0$ and $\xi \to 0$, it follows that $u_{ql} \to u \to 0$, and the series, expressed in Equation 16, is reduced to the result of Equation 17.3 in the following way for an infinite stack:

$$x = 1 - u, \qquad (17.1)$$

$$\sum_{s=0}^{\infty} x^s = \frac{1}{1-x}, \quad x < 1\,, \qquad (17.2)$$

$$u_{s\infty} = \lim_{u\to 0^+}\left[u\sum_{s=0}^{\infty}(1-u)^s\right] = \lim_{x\to 1^-}\left[(1-x)\sum_{s=0}^{\infty}x^s\right] = \lim_{x\to 1^-}\left(\frac{1-x}{1-x}\right) = 1, \qquad (17.3)$$

where the changes of variables were done: $1-u = x$ and $s = q - 1$ and used the convergence of the series of Equation 17.2. The important result is that only an infinite stack in such reversible conditions can achieve a stack utilization $u_{s\infty}$ of 1 (Equation 17.3).

Moreover, we can intuitively assert that the stack utilization must be:

$$u_{sn} = n\frac{iA}{(c/v_l)\dot{n}^i_{1l}F} = \xi_{sn}, \qquad (18.1)$$

i.e. the stack utilization u_{sn} is n-fold the utilization of one cell, because in every cell the same amount of reagent is utilized to keep the same current in the stack.

Using Equations 5 and 18.1, an efficiency definition is obtained for a steady state, depending on the whole stack reaction extent ξ_{sn}:

$$\eta = \frac{\dot{W}_{\mathrm{el}}}{\dot{H}_{\mathrm{P}} - \dot{H}_{\mathrm{R}}} = \lim_{n\to\infty} \frac{iA}{\frac{1}{v_l}\dot{n}_{1l}^{in}\left(\sum v_p h_p - \sum v_r h_r\right)}$$
$$= \lim_{n\to\infty} \frac{u_{sn}\frac{1}{n}\sum_{q=1}^{n} U_q F(c/v_l)}{\frac{1}{v_l}\left(\sum v_p h_p - \sum v_r h_r\right)}$$
$$= \lim_{n\to\infty} \frac{u_{sn}\overline{U}F(c/v_l)}{\frac{1}{v_l}\left(\sum v_p h_p - \sum v_r h_r\right)} = \lim_{n\to\infty} \frac{\xi_{sn} c\overline{U}F}{\sum v_p h_p - \sum v_r h_r}$$
$$= \lim_{n\to\infty} \frac{c\overline{U}F\xi_{sn}}{\Delta H}, \qquad (18.2)$$

where $\sum_{q=1}^{n} U_q$ is the total stack potential, $\overline{U}$ is the average stack potential, ξ_{sn} is the stack reaction extent identical to u_{sn}, h_p and h_r are the molar enthalpy of products p and the molar enthalpy of reagents r, respectively. For a reversible infinite stack this equation takes the following form, which considers the result obtained in Equation 17.3:

$$\eta_{s\infty} = \lim_{n\to\infty} \frac{c\overline{U}F\xi_{sn}}{\Delta H} = \frac{c\overline{U}(\xi_q = 0)F \cdot 1}{\Delta H} = \frac{U(0)}{U_H} = \frac{\Delta G}{\Delta H}, \qquad (19)$$

where $U(0)$ is the potential of one cell at reaction extent $\xi_q = 0$ and it coincides with the average potential $\overline{U}$ in conditions of reversibility. Equation 19 resembles Equation 1, which is the limit case, corresponding to an Infinite Reversible Fuel Cell Stack in standard conditions. It is noteworthy that, although we start with operative conditions, steady state leads to time independent equations like Equations 18.2 and 19.

4. The irreversible stack

4.1. *Model definitions for Chain Flow*

The irreversible stack efficiency has the same definition as in Equation 18.2, without the limit operator. However, in this case, the numerator is an irreversible power and $\bar{U}$ must be found through models. This implies the need to determine the reaction extent, the flow rates and the partial pressures of each cell previously, hence the potential of each cell and the average potential in a Chain Flow stack.

The first step consists of noting that there is a series of equalities between the product of the utilization and the inlet flow rate of each cell:

$$u_{1j}\dot{n}_{1j} = u_{2j}\dot{n}_{2j} = .. = u_{qj}\dot{n}_{qj} = .. = u_{nj}\dot{n}_{nj} = \frac{v_j i A_q}{cF} = v_j\dot{\xi} \qquad (20)$$

from which is obtained:

$$\frac{u_{qj}}{u_{q+1,j}} = \frac{\dot{n}_{q+1,j}}{\dot{n}_{qj}} \qquad (21)$$

and from the definition of utilization of Equation 6 it is shown that:

$$u_{qj} = 1 - \frac{\dot{n}_{q+1,j}}{\dot{n}_{qj}} \qquad (22)$$

combining Equations 21 and 22, gives

$$u_{q+1,j} = \frac{u_{qj}}{1 - u_{qj}}. \qquad (23)$$

Introducing u_{1j} in the Equation 23 for u_{2j} and so on iteratively, the following general equation is achieved:

$$u_{q+1,j} = \frac{u_{1j}}{1 - qu_{1j}}; \quad qu_{1j}<1 \qquad (24)$$

and since the products of flow rates with the corresponding utilizations are constant (Equation 20), the flow rate can be expressed as:

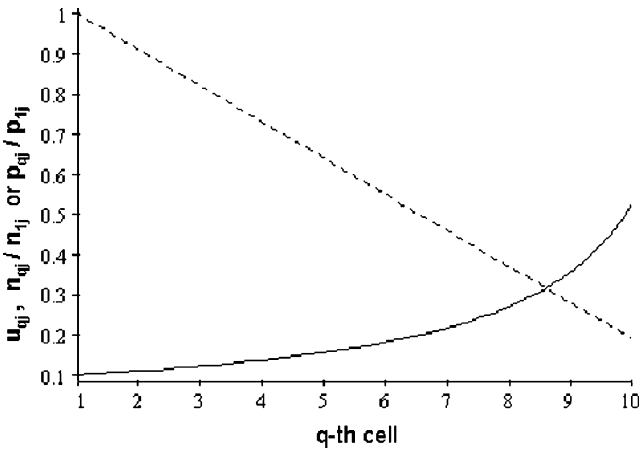

Fig. 2. Utilization (solid line), flow rate and pressure trends (dotted line) calculated by Equations 24, 25 and 26. The initial utilization $u_{1j} = 0.09$.

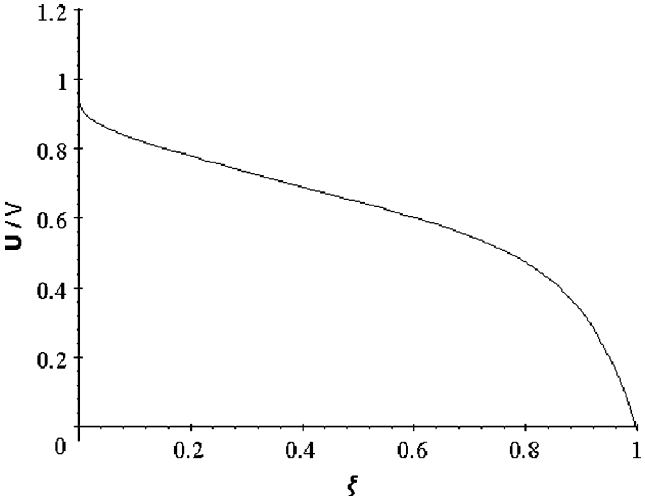

Fig. 3. Polarization curve, temperature 298 K, pressure of gases 100 kPa, oxygen flow rate 9.37×10^{-5} mol-O_2 s^{-1} and hydrogen flow rate 1.12×10^{-4} mol-H_2 s^{-1}.

$$\dot{n}_{q+1,j} = \dot{n}_{1j}(1 - qu_{1j}); \quad qu_{1j} \leq 1. \tag{25}$$

Flow rates and cell utilizations are reported in Figure 2, for $u_{1j} = 0.09$ and a 10 cell stack, where the hyperbolic increment of utilization and the linear decrement of flow rates are evident.

Partial pressures should follow a similar behavior to the molar flow rates (Figure 2), for the ideal gas state equation, considering that the stack volume and temperature are constant and neglecting friction of gases in the flow fields:

$$p_{q+1,j} = p_{1j}(1 - qu_{1j}); \quad qu_{1j} \leq 1. \tag{26}$$

The global utilization of a stack would take the following form, combining Equations 16 and 24:

$$\begin{aligned} u_{sn} &= u_{1l} + \frac{u_{1l}}{1 - u_{1l}}(1 - u_{1l}) + \cdots \\ &= nu_{1l} = \frac{inA}{(c/v_l)\dot{n}_{1l}F} = \xi_{sn}. \end{aligned} \tag{27}$$

The stack utilization is n-fold utilization of the first cell, for a stack of identical cells, as asserted in Section 3 for the reversible case. It is noteworthy that the definition of $u_{sn} = n \cdot u_{1l}$ is useless to solve the reversible case, because we obtain the indetermination $u_{s\infty} = \infty \cdot 0$; nor can we solve it supposing that $u_{sn} = 1$ and so obtaining n if $u_{1l} = 0$, because u_{sn} is what we are looking for in an infinite stack.

The efficiency definition, seen in Section 3, is used without the limit case [12]:

$$\begin{aligned} \eta = \frac{\dot{W}_{\text{el}}}{\dot{H}_{\text{P}} - \dot{H}_{\text{R}}} &= \frac{iA\sum_{q=1}^{n} U_q}{\frac{1}{v_l}\dot{n}_{1l}\left(\sum v_p h_p - \sum v_r h_r\right)} \\ &= \frac{c\left(\frac{1}{n}\sum_{q=1}^{n} U_q\right)Fu_{sn}}{\sum v_p h_p - \sum v_r h_r} = \frac{c\overline{U}F\xi_{sn}}{\Delta H}, \end{aligned} \tag{28.1}$$

where we have carried out a substitution, considering the following equality obtained from Equation 27:

$$\frac{iA}{\frac{1}{v_l}\dot{n}_{1l}} = \frac{cFu_{sn}}{n}. \tag{28.2}$$

It is necessary to state that in this model we are supposing that temperature is uniform and all transformations are carried out at a constant temperature, as Equations 12.5, 12.6, 25 and 26 require. The assumption of constant temperature is valid if a cooling system acts as a thermostat for a stack working for a long period. It is also be valid for short times of operation, during which there is not enough time to create relevant temperature gradients along the stack, but the dependence of the coefficients α_i (Equations 12.2, 12.3 and 13) on temperature can be made explicit whether needed or not.

It is necessary to start from a polarization curve, and the model proposed within Equations 12.1–13, to manage Equation 28.1. The polarization curve reported

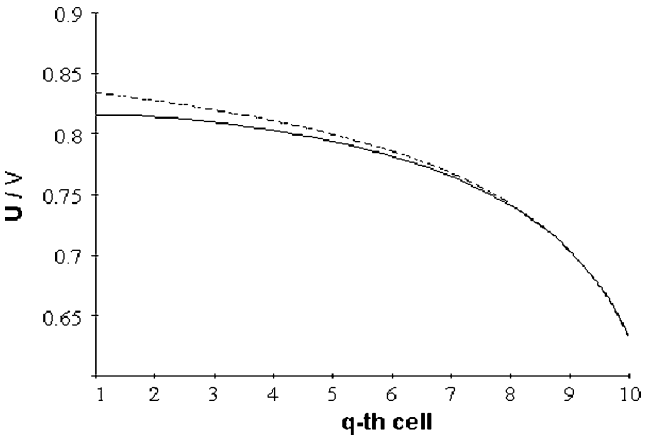

Fig. 5. Cells potentials for parallel flows (dotted line) and counter flow (solid line); $u_{1l} = 0.09$ for both cases.

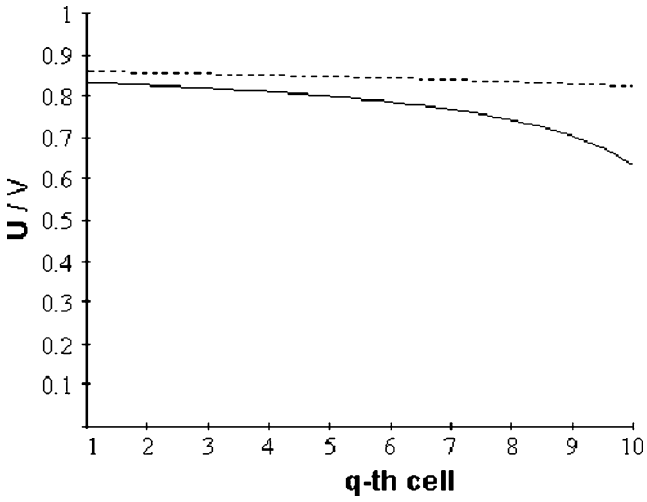

Fig. 4. Cells potentials of a stack of 10 cells, solid curve: $u_{1l} = 0.09$, dotted curve $u_{1l} = 0.05$.

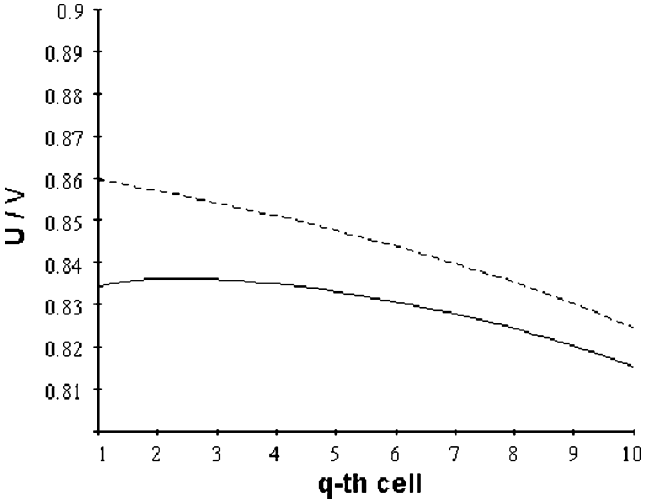

Fig. 6. Cells potentials for parallel flows (dotted line) and counter flow (solid line); $u_{1l} = 0.05$ for both cases.

in Figure 3 was used in order to do various calculations and predictions. This curve was obtained from a SZW (Zentrum für Sonnenenergie-und-Wasserstoff-Forschung) Protonic Exchange Membrane (PEM) single fuel cell, with active area A of 100 cm^2, tested by means of the FCATS screener test station by Hydrogenics Co. at the University of Applied Sciences of Stralsund, Germany. The test conditions were: cell temperature of 298 K, air flow rate of 600 ml min^{-1} (9.37×10^{-5} mol-O_2 s^{-1}), hydrogen flow rate 150 ml min^{-1} (1.12×10^{-4} mol-H_2 s^{-1}), where the limiting reagent was hydrogen, the pressure of both gases was 100 kPa, and the humidity 35%. The equation describing this polarization curve is:

$$U(\xi, 100\ \text{kPa}, 298\ \text{K}) = 0.826 - 0.378\xi - 0.0176 \ln \xi - 1.0077 \times 10^{-5} \exp(10.74\xi). \quad (29)$$

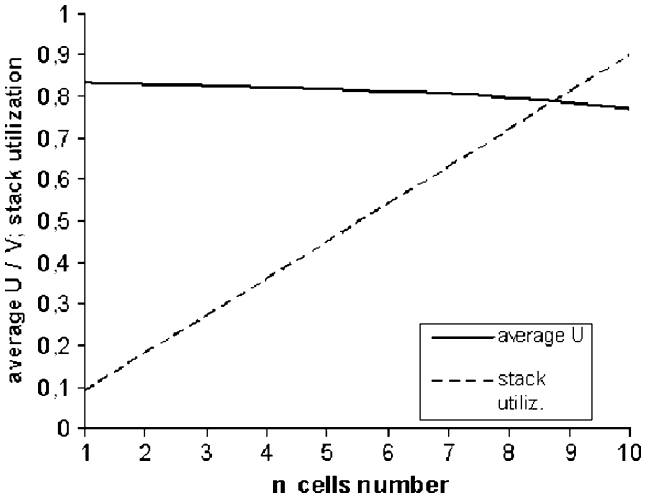

Fig. 7. Average stack potential $\bar{U}$ and stack utilization (u_{sn}) with increasing total cells number n ($u_{1l} = 0.09$).

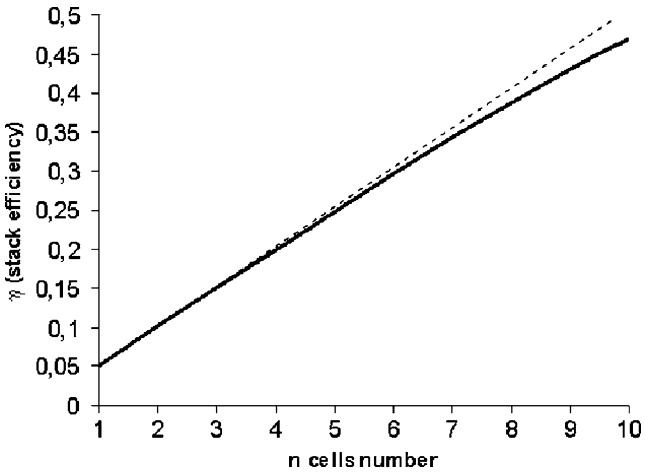

Fig. 8. Stack efficiency (solid line) compared with linear behavior (dotted line), $u_{s10} = 0.9$.

This polarization curve is a useful tool to do various calculations, for instance, other curves can be used without affecting of the general results. Applying Equation 23, where u_{ql} is taken as the reaction extent ξ_q (Equation 10), and Equations 26 and 29 in Equations 12.1–12.4, the potential of each cell can be forecast. In Figure 4, the cell potentials of a stack of 10 cells in two different situations are shown. In the former, the first cell reaction extent is of 0.09 and in the latter 0.05. The temperature is considered constant at 298 K, for the steady state conditions, and uniform in the whole stack. Water drag is also supposed to be efficient and friction effects of gaseous reagents are neglected. The term α_6 of Equation 12.2 is taken as 0.013 V, corresponding to the value of RT/cF for $c = 2$. The potential decay is faster in the case where there is higher first cell utilization ($u_{1l} = 0.09$) (Figure 4).

The assumption of uniform temperature is important because the effect of counter flow of reagents, which could be confused with the effect of temperature, can be clearly observed.

Another important case to be considered is one in which flows are in opposite directions. In such a situation, the pressure of the gas in counter flow can be so expressed:

$$p_{q-1,j} = p_{nj} q u_{nj} \quad (30)$$

In Equation 30, u_{nj} is the lowest utilization and p_{nj} the highest pressure for reagent j, which is in counter flow. The effect of counter flow is very slight when the first cell utilization u_{1l} is high (0.09) and its effects are manifested overall in an initial cell potential decay (Figure 5). With lower utilizations of the first cell ($u_{1l} = 0.05$ in the example) the effect of counter flow is not only an initial potential decay, but also the presence of a potential maximum along the cell stack. In our example, the maximum is in the third cell (Figure 6); nevertheless, counter flow cell potentials are always lower than those of parallel flows (Figures 5 and 6).

4.2. *Efficiency determination for Chain Flow case*

The average potential $\overline{U}$ is calculated using the equation:

$$\overline{U}(n) = \frac{1}{n} \sum_{q=1}^{n} U(\xi_q, T, p_{qj}). \quad (31)$$

Considering a fixed and uniform temperature along the stack, a fixed initial gas pressure p_{1j} and fixed ξ_1, the only real variable is the number of cells n. The average potential $\overline{U}(n)$ and stack utilization u_{sn} are shown in Figure 7, for the case of parallel flow, and for a maximum of 10 cells per stack and initial first cell utilization $u_{1l} = 0.09$. The average potential decreases slightly with an increase in the number of cells. For this reason, the efficiency doesn't grow linearly but has a

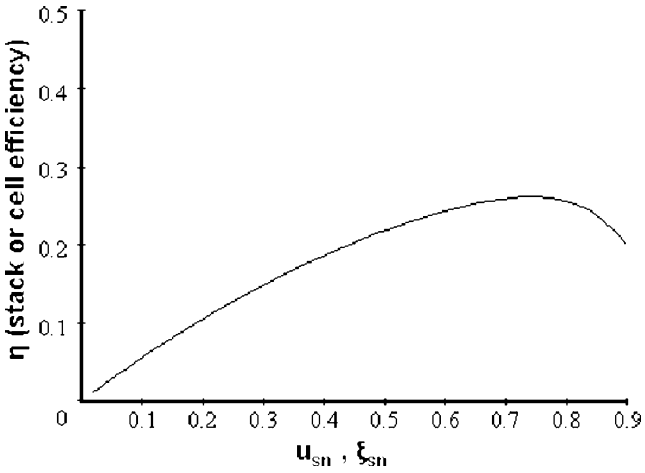

Fig. 9. Stack or cell efficiency of Separate Flow case.

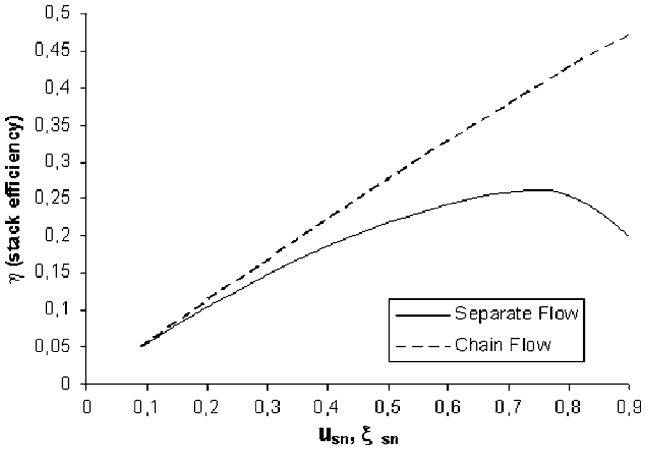

Fig. 10. Comparison of efficiencies of both Chain Flow and Separate Flow stacks. Note that 1 cell corresponds to $u_{s1} = 0.09$ and 10 cells stack corresponds to $u_{s10} = 0.9$.

slight deflection from linearity, which is more accentuated when stack utilization approaches 1 (Figure 8). The achieved efficiency, calculated by Equation 28, is 0.47 for a 10 cell stack and a very high stack utilization of 0.9 ($U_H = 1.48$ V, $\triangle H = \triangle H^\circ = -285.5$ kJ).

4.3. *Efficiency determination for Separate Flow case*

In the Separate Flow case, the main flow rate $\dot{n}_j$ is divided into n equal flow rates:

$$\dot{n}_{qj} = \frac{\dot{n}_j}{n}. \tag{32}$$

The stack utilization for the limiting reagent coincides with the cell utilization:

$$u_{sn} = \xi_{sn} = \frac{\dot{n}_l^{\text{in}} - \dot{n}_l^{\text{out}}}{\dot{n}_l^{\text{in}}} = \frac{n(\dot{n}_{\text{ql}}^{\text{in}} - \dot{n}_{\text{ql}}^{\text{out}})}{n\dot{n}_{\text{ql}}^{\text{in}}} = u_{\text{ql}} = u_l = \xi. \tag{33}$$

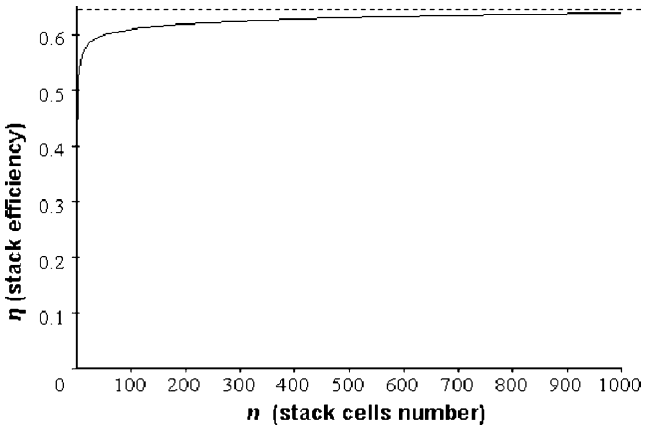

Fig. 11. Fuel cells stack efficiencies with increasing total cells' number (stack utilization $u_{sn} = 0.9$). Dotted straight line: efficiency of an infinite stack.

The cell utilization can also be written in the following form:

$$u_l = \frac{iA}{\frac{c}{v_l}\left(\frac{\dot{n}_l}{n}\right)F} = \frac{\text{in}A}{\left(\frac{c}{v_l}\right)\dot{n}_l F}, \tag{34}$$

implying that at a given current density i and $\dot{n}_l$, the cell utilization is proportional to the number of cells n which composes the stack.

The potential of each cell must be also the same:

$$U(q) = U. \tag{35}$$

The efficiency is thus defined, taking into account Equations 34 and 35:

$$\eta_s = \eta_q = \frac{cFU\xi}{\Delta H} \tag{36}$$

indicating that the stack efficiency η_s is equal to the cell efficiency η_q. The efficiencies of stacks, whose behavior strictly follows the Separate Flow conditions as established, do not depend on the number of cells, but only on utilization. Using the same polarization curve and operative conditions described in Subsection 4.1, the efficiency manifests the behavior shown in Figure 9, where a maximum efficiency of approximately 0.26 is present, with a reaction extent of about 0.75. A comparison between Chain Flow and Separate Flow stack efficiencies is shown in Figure 10, using the common abscissa variable i.e. the reaction extent ξ_{sn}. Only at low utilization is the behavior of efficiencies of both cases quite similar, and then it diverges (Figure 10). Efficiency of Chain Flow stacks has a slight decline at high stack utilization; however, since Separate Flow stacks follow the efficiency behavior of a single cell, their efficiency decay is very pronounced at high utilization.

4.4. *Efficiency variation and number of cells*

By extrapolating the linear behavior of efficiency at low utilizations, as shown in Figure 8 for the Chain Flow case, the efficiency of 0.56 for 10 cells stack is obtained, with stack utilization $u_{s10} = 0.9$, i.e. it is overestimated. Nevertheless, by keeping this linear behavior with the derivative of the straight line coinciding to $U_{1l}(\xi_1)$ (Equation 12.3), it can be estimated how efficiency varies incrementing total number of cells of the stack n (every stack has utilization of 0.9 and first cell utilization u_{1l} is $0.9/n$). In Figure 11, the efficiency variation with n can be observed; in this representation, efficiencies at high n are emphasized, because at low n there is a discrepancy, as stated above. Efficiency first increases quickly with n, and then slowly, this suggests that at high efficiencies more and more cells are needed to approach the reversible limit. The efficiency limit (shown with the dashed line and corresponding to 0.645) is the value obtained from experiments in the reversible case, i.e. it has been calculated by the potential of a single cell without current, $U(0) = 0.955$ V (in the conditions described in Section 4.1) and by Equation 19.

5. Discussion

This work deals with the definition, calculations and predictions of efficiencies of fuel cells. Its aim is to forecast, or estimate, efficiencies of stacks from the characteristics of single cells. A polarization curve, obtained in defined conditions, can be represented by means of phenomenological models (Equations 12.1–12.6). This curve can be reported as a function of the dimensionless variable called utilization. Moreover, reaction extent, another dimensionless variable, can be defined both for each cell (Equation 10) and for the whole stack (Equation 27), assimilating it with the utilization of the limiting reagent. The appropriate variable would be the reaction extent (Equation 10), because it refers directly to the reversibility of the process and commonly used in thermodynamics. These terms are used with some latitude; when speaking of the utilization of the limiting reagent, according to the stated definitions, the two terms coincide. In the model for the polarization curve (Equations 12.1–12.6 and 13), as described by the dimensionless variable reaction extent, the grade of irreversibility of the process is considered, since reaction extent increases, the irreversibility does also and the potential consequently decays. The coefficients α_2, α_3, α_4, α_5, α_6 of this model include several effects of the irreversible phenomena occurring in the fuel cell: activation, ohmic and concentration polarizations, and humidity effects. Considering that each cell of a stack has its own reaction extent, the model can be used to predict cell potentials. In the Chain Flow stack, the reversible and the irreversible cases are distinguished. In the reversible case, only an infinite stack can satisfy the requirement of an infinite series of equilibrium states through the entire process. In this case, the reaction rate $\dot{\xi}$ (Equation 9) tends to 0 and the efficiency is reduced to the ratio of the potential of a single cell without load, with the potential extrapolated from enthalpy U_H (Equation 19). In the reversible case, Chain Flow and Separate Flow tend to coincide. This is true because each cell utilization tends to be the same $u_{ql} \rightarrow u$, in the reversible case, which is equivalent to that expressed in Equation 33 for the Separate Flow.

In the irreversible case, the cell potential decays as the number q of the cell increases in the series, as shown in Figure 4. This decay is more accentuated in the case of high stack utilization, due mainly to hyperbolic increase of cell utilization (Figure 2). Moving from the first cell, the process is more irreversible and the several overpotentials become larger; consequently the potential decays. The flows of the two reagents can be carried out in parallel, or in opposite directions. The effect of counter flow is more evident with low utilizations, where it generates the appearance of a potential maximum along the stack; in any case, counter flow causes a lowering of the potential of the initial cells (Figures 5

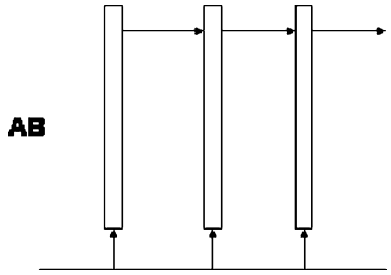

Fig. 12. Flow path of a stack where a main feeding flow is divided among all the cells and the outlet flows are collected in one stream. AB is the case between cases A and B, described in Figure 1. Each cell is represented by a box and each flow path by an arrow.

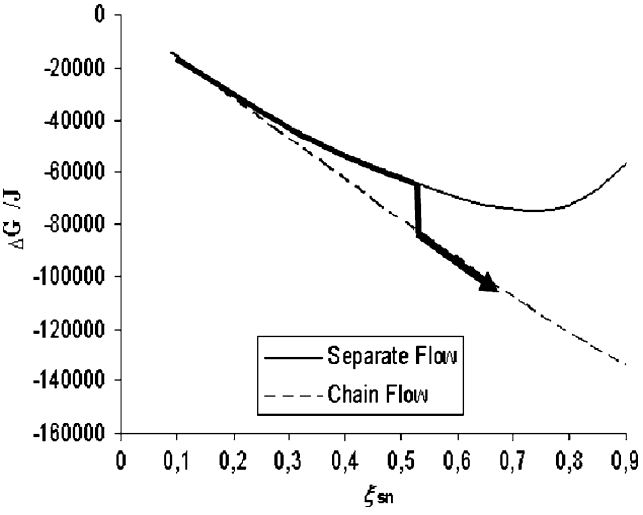

Fig. 13. Gibbs free energy ΔG variation with reaction extent ξ_{sn} for Chain (n varies from 1 to 10 and $u_{1l} = 0.09$) and Separate Flow stacks. The bold arrow indicates a possible transition from one dominant behavior to the other with lower Gibbs free energy.

and 6). The introduction of a temperature gradient into the model would not allow the identification of the effect of counter flow on potential.

The efficiency has been determined for an initial cell utilization $u_{1I} = 0.09$ and for stacks up to a maximum of 10 cells. Calculations show that a larger stack is more efficient; however, the increment of efficiency is not linear, because the average potential of the stack declines, with increasing the total number of cells n (Figures 7 and 8).

In the Separate Flow stacks, the problem is easier, because the reaction extent of each cell is the same, and is equal to the stack reaction extent; for this reason, the efficiency of the stack is a function only of reaction extent ξ. The efficiency shows a maximum, in our case $\eta \approx 0.26$ at ξ 0.75 (Figure 9), a significantly low efficiency, compared with the Chain Flow case. A direct comparison of Chain and Separate cases, using the common variable of reaction extent, reveals that, at low reaction extents, the two cases are very similar and then they diverge. Finally, efficiency decline is accentuated in the Separate case (Figure 10), because all cells have the same low potential with high utilizations, while in the Chain case only, the ending cells have low potentials. In this case, the irreversibility of the process grows along the stack.

The question is how efficiency can be improved, keeping the reaction extent of the stack for the Chain Flow case constant; for example, at $\xi_{sn} = 0.9$ and changing the stack total number of cells n. A tentative answer is given in Figure 11, although efficiency is overestimated at low n, it rises with n, but its increment decreases with s of n increment. In brief, the increment of η, with respect to that of n is always positive, but tends to vanish:

$$\left(\frac{\delta\eta}{\delta n}\right)_{\xi} > 0 \tag{37}$$

$$\lim_{n\to\infty}\left(\frac{\delta\eta}{\delta n}\right)_{\xi} = 0 \tag{38}$$

Equations 37 and 38 are not true derivatives, because the function displayed in Figure 11 is a discrete function, n being an integer number so that δ only represents a variation whose lowest value is 1. However, Equation 38 tells us that the limit efficiency, represented by the reversible and infinite stack, is approached asymptotically.

A large portion of the real fuel cell stacks are not exactly Chain Flow or Separate Flow stacks, but are, in general, a combination of both, as shown in the scheme of Figure 12. A main feeding stream is divided among the cells and all the outlet streams are recollected in one main stream (case AB in Figure 12). In some circumstances a behavior of Chain or Separate stacks would predominate. As suggested by Figure 10, Chain behavior must be thermodynamically favored at high utilizations, because higher power efficiency means lower Gibbs free energy (Figure 13). A transition from one dominant behavior to the other may be possible, as schematically indicated by the bold arrow in Figure 13. If the reaction extent of the stack is increased, gases would probably follow a flow rates profile such as the one shown in Figure 2, where a gradient of reagent flow rates is present along the stack.

6. Conclusions

The definition of efficiency, based on operative parameters for steady states, leads to a time-independent efficiency definition, where reversible or irreversible Gibbs free energy change appears in the numerator, and reversible enthalpy of reaction in the denominator (Equation 28).

The use of such a definition implies that the potential and reaction extent of each cell of a stack can be predicted. The capacity to predict electrical behavior of stacks, made by identical cells, depends essentially on the model used for the polarization curve of a single cell and the chosen variables. The dimensionless reaction extent is a suitable variable to correlate potential variation with cell number, and to be used in thermodynamics. The chosen model for the proposed polarization curve was developed by Kim et al. [9], where a term was added to take in account the drop of partial pressures along the stack. The highest efficiency resulted in a reversible Chain Flow infinite stack (Equation 19), whose reaction rate tends to be null. The Chain Flow case allows the achievement of higher efficiencies, which increases with total number of cells n, although cell and average potentials decrease (Figures 7 and 8). The efficiency, at a fixed stack reaction extent, rises with the total stack number of cells n, but each new equal increment of efficiency needs more cells to be carried out, i.e. to reach the reversible limit, an infinite number of cells will be necessary (Figure 11). On the other hand, a rigorous Separate Flow does follow the efficiency of single cells (Figure 9). Stacks usually have a combination of Chain and Separate Flow behavior (Figure 12), meaning that a large stack with many cells will be more efficient of a small stack, and that 'Chain behavior' is thermodynamically favored overall at high stack utilizations (Figure 13).

References

1. A.E. Lutz, R.S. Larson and J. Keller, *Int. J. Hydrogen Energy* **27** (2002) 1103.
2. A. Kazim, *Energy Conversion Manage.* **45** (2004) 1949.
3. Y.A. Cengel and M.A. Boles, 'Thermodynamics – An Engineering Approach', 2nd ed (McGraw-Hill, Inc., 1994).
4. P.F. Oosterkamp, A.A. Goorse and L.J. Blomen, *J. Power Sources* **41** (1993) 239.

5. K. Kordesch and G. Simader, 'Fuel Cells and Their Applications', (VCH, 1996).
6. E. Chen, *in* Gregor Hoogers (Ed.), 'Fuel Cell Technology Handbook' Chapter 3, (CRC Press LLC, 2003), pp. 3.1–3.30.
7. A. Weber, R. Darling, J. Meyers and J. Newman, *in* Handbook of Fuel Cells, Fundamental Technology and Applications, Vol.1, Chapter 7, (Ed. Wiley, 2003), pp. 47–69.
8. J. Bockris and S. Srinivasan, 'Fuel Cells: Their Electrochemistry', (McGraw Hill, New York, 1969).
9. J. Kim, S.M. Lee, S. Srinivasan and C.E. Chamberlin, *J. Electrochem. Soc.* **142** (1995) 2670.
10. T.E. Springer, T.A. Rockward, T.A. Zawodzinski and S. Gottesfeld, *J. Electrochem. Soc.* **148**(1) (2001) A11.
11. J. Newman, *Electrochim. Acta* **24** (1979) 223.
12. A.K. Demin, P.E. Tsiakaras, V.A. Sobyanin and S.Yu. Hramova, *Solid State Ionics* **152–153** (2002) 55.